



**HAL**  
open science

## Modeling and sizing the coil in boost converters dedicated to photovoltaic sources

Lotfi Atik, Mohammed Amine Fares, Jean Zaraket, Ghalem Bachir, Michel  
Aillerie

► **To cite this version:**

Lotfi Atik, Mohammed Amine Fares, Jean Zaraket, Ghalem Bachir, Michel Aillerie. Modeling and sizing the coil in boost converters dedicated to photovoltaic sources. TMREES18-Spring Meeting "Technologies and Materials for Renewable Energy, Environment and Sustainability", Feb 2018, Beirut, Lebanon. pp.30084 - 30084, 10.1063/1.5039271 . hal-01802886

**HAL Id: hal-01802886**

**<https://centralesupelec.hal.science/hal-01802886>**

Submitted on 5 Jun 2018

**HAL** is a multi-disciplinary open access archive for the deposit and dissemination of scientific research documents, whether they are published or not. The documents may come from teaching and research institutions in France or abroad, or from public or private research centers.

L'archive ouverte pluridisciplinaire **HAL**, est destinée au dépôt et à la diffusion de documents scientifiques de niveau recherche, publiés ou non, émanant des établissements d'enseignement et de recherche français ou étrangers, des laboratoires publics ou privés.

## **Modeling and sizing the coil in boost converters dedicated to photovoltaic sources**

Lotfi Atik, Mohammed Amine Fares, Jean Zaraket, Ghalem Bachir, and Michel Aillerie

Citation: [AIP Conference Proceedings](#) **1968**, 030084 (2018); doi: 10.1063/1.5039271

View online: <https://doi.org/10.1063/1.5039271>

View Table of Contents: <http://aip.scitation.org/toc/apc/1968/1>

Published by the [American Institute of Physics](#)

---

---

# Modeling and Sizing the Coil in Boost Converters Dedicated to Photovoltaic Sources

Lotfi Atik<sup>1,2,3,4,a)</sup>, Mohammed Amine Fares<sup>1,2,3,4</sup>, Jean Zaraket<sup>3,4</sup>,  
Ghalem Bachir<sup>1,2</sup>, and Michel Aillerie<sup>3,4,b)</sup>

<sup>1</sup>University of science and technology of Oran, USTO, LDDE, Oran, Algeria.

<sup>2</sup>Laboratoire de Développement Durable de l'Energie Eclectique (LDDEE)

<sup>3</sup>Université de Lorraine, LMOPS, EA 4423, 57070 Metz, France.

<sup>4</sup>CentraleSupélec, LMOPS, 57070 Metz, France.

<sup>a)</sup>Corresponding author : [lotfiatik31@gmail.com](mailto:lotfiatik31@gmail.com),

<sup>b)</sup>[aillerie@metz.supelec.fr](mailto:aillerie@metz.supelec.fr)

**Abstract.** The coil is a very important element in a wide range of power electrical systems as such as those used in converter or inverter dedicated to extract and to adapt the value and the shape of the intensity and the voltage delivered by renewable energy sources. Thus, knowing its behavior in converters is paramount to obtain a maximum conversion efficiency and reliability. In this context, this paper presents a global study of a DC/DC boost converter dedicated to photovoltaic sources based on the modeling of the behavior of the coil or the inductance as a function of the switching frequency.

**Index Terms.** Photovoltaic systems, Magnetic Coil, Boost Converter.

## INTRODUCTION

In electromagnetic systems, only the magnetic energy is likely to be stored in enough density to be converted into another form of energy, in large quantities. Thus, in such system, the magnetic circuit is the central element of the converter as it assumes the storage and the transformation [1].

The coils can serve as a controlled switch in the context of the magnetic regulation. This one is a method of regulating a power electronics converter that uses the properties of saturable inductors. In fact, an inductance in its linear functioning zone  $B(H)$  which is a relation between flux density and the magnetic field, it's generally used so that it doesn't change its value, which is particularly important for maintaining fixed cutoff frequency of a filter.

Coils have an essential impact in different applications. They are used as electric current transformers to transform high current values in the kilo-ampere range to low ones or contrary. They are also inserted in power electrical network as galvanic isolation transformers. We can also found coils used to transform a neutral system, in which the transformer neutral and the materials masses are common and connected to the ground, into isolated ground systems for supplying loads and apparatus sensitive to disturbances. Another important family of applications for coils is their used for various functions consisting to eliminate parasites of analog signals providing from power generators, thus playing the role of impedance. In environmental application, they are also used in magnetic and electronic ballasts for discharge lamp lighting i.e. the fluorescent lamps, metal halide lamps, etc. For medicine, coils are integrated in medical apparatus like magnetic resonance imaging. For that application, the most commonly used magnets are superconducting electromagnets. They consist of a coil made superconducting by cooling liquid helium, surrounded by liquid nitrogen. They allow to obtain intense and homogeneous magnetic fields but are expensive and must be maintained regularly. Finally, as straightforwardly concerned by the current contribution, coils constitute the main basic element of DC/DC boost converters inserted in an electric generator to convert the DC power produce by a source, here dedicated to renewable energy sources, specially photovoltaic, to DC current and voltage adapted to final applications.

In previous contributions, authors of our research group have presented a specific topology of DC/DC magnetically boost converter and their associated maximum power point tracker [2,3]. The topology of the converter was a boost based on an inductor at its input. Even if the main objective of these primary contributions was elsewhere, the important role of the coil in DC/DC converters was considered but not modeled and the fundamental importance of its sizing was not enlighten and evaluated. Nevertheless, this studied topology of converter proven its effectiveness in energy conversion and it was once again chosen for the current study here reported. Indeed, in this paper we focus on the sizing of inductor L dedicated to boost converters, then, in the objective of optimization of the energy conversion process, and we present the successive steps to follow for optimizing a coil based on real results.

## THE TWO EXISTING MODELS OF COILS

Starting with general considerations and basics, a coil, or auto-inductor is a common component in electrical engineering and electronics as mentioned in the introduction with a non-exhaustive list of applications. A coil consists of a winding of a conductive wire of N-turn windings around a ferromagnetic core material called "ferrite core" [4,5]. The magnetic field is a manifestation of the energy. The coil receives electrical energy and transforms it into magnetic energy. As it is well known by students since their first lesson of electronic, the flux produced by a coil is proportional to the current flowing through it, and the coefficient of proportionality is called "inductance" whose symbol is L. A torical coil with its pertinent relative electrical parameters is represented in Fig. 1.

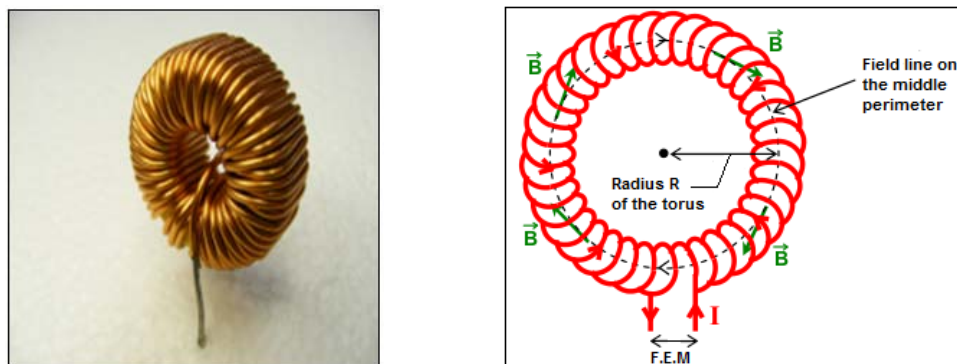


Figure 1. A torical coil.

The stored electromagnetic energy has the usual form expressed by

$$E = \frac{1}{2} Li^2 \quad (1)$$

The ideal coil [6] is modeled by a self-inductance denoted generally L. A real coil, especially when it is wound around a ferromagnetic material, is a complex dipole with many parameters at the origin of physical phenomena inducing nonlinearities. The simplest and most frequently used models of real coil are those corresponding to the combination of an inductance and a resistor. They are grouped in the dipole model family.

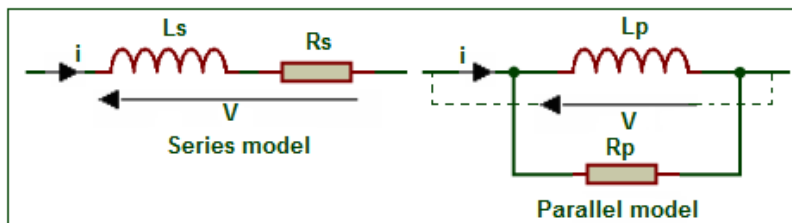


Figure 2. Dipole models (series, parallel).

The series dipole model consists of the series connection of an inductance coil and a resistor. It corresponds to the following formula:

$$V = Ls \cdot \frac{di}{dt} + R_s \cdot i \quad (2)$$

The second one, i.e. the parallel dipole model consists of the parallel association of an inductance coil and a resistor. It corresponds to the following formula:

$$i = \frac{1}{L_p} \int_T u dt + \frac{V}{R_p} \quad (3)$$

Finally, a more general model, constituted by a combination of the two previous ones describes more closely the behavior of a coil as it will take into consideration the both parasitic resistances. It is represented in Fig. 3.

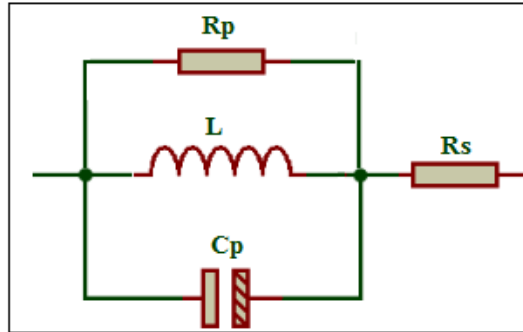


**Figure 3.** Equivalent model of impedance  $Z(\Omega)$ .

Knowing that  $C_p$  ( $\mu F$ ) is the parasitic capacitance due to connection wires and inter-turns capacitance,  $R_s$  ( $\Omega$ ) is the parasitic resistance series due to connection wires and winding,  $R_p$  ( $\Omega$ ) is the parallel parasitic resistance linked to magnetic losses, and finally,  $L$  (H) is the inductance.

## THE BASIC BOOST CONVERTER

The voltage provided by photovoltaic panels is generally not adapted to the voltage required by the loads even if the photovoltaic source is sizing to respond in terms of power. Combine several photovoltaic panels in series and parallel to build a PV field is not the solution generally adopted because it isn't suitable to extract the maximum power of the primary available energy and to keep constant the output voltage of the photovoltaic power plant. Using power electronics, there are several static converter topologies that can serve this demand. Boost or parallel converters are in this category of static converter and was shown as an efficient powerful solution [7,8]. Such converter is shown on Fig. 4, in its simplest basic form when the switch is assumed by a MOSFET.

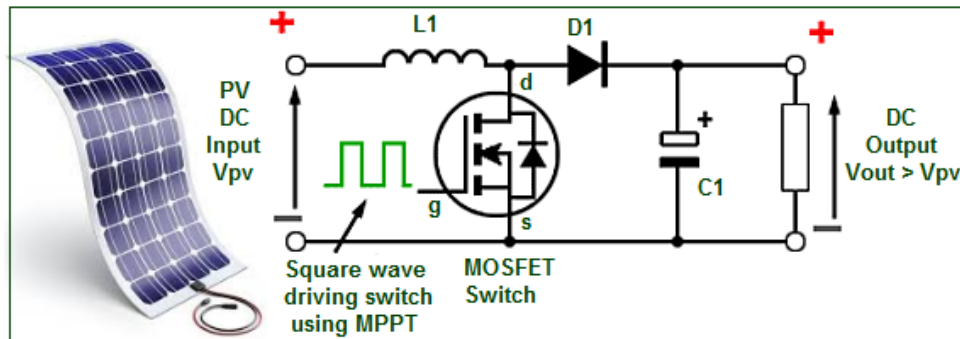


**Figure 4.** Equivalent electrical circuit of boost converter.

A boost converter [9-11] (step-up converter) is a DC-to-DC power converter that steps up the voltage, of course while stepping down current to assume a constant power, from its input, i.e. the supply to its output, i.e. the load. It is a class of switched-mode power supply (SMPS) containing at least two semiconductors, a diode and a transistor and at least one energy storage element: a capacitor, inductor, or the two in combination. To reduce

voltage ripple, filters simply made with capacitors or in combination with inductors are normally added at the input of the converter as supply-side filter, or at its output as load-side filter. The key principle that drives the boost converter use the basic properties of the inductor that opposes to the changes of the current, a change in the magnetic field.

The boost converter works in two different modes during one cycle as shown on Fig. 5.

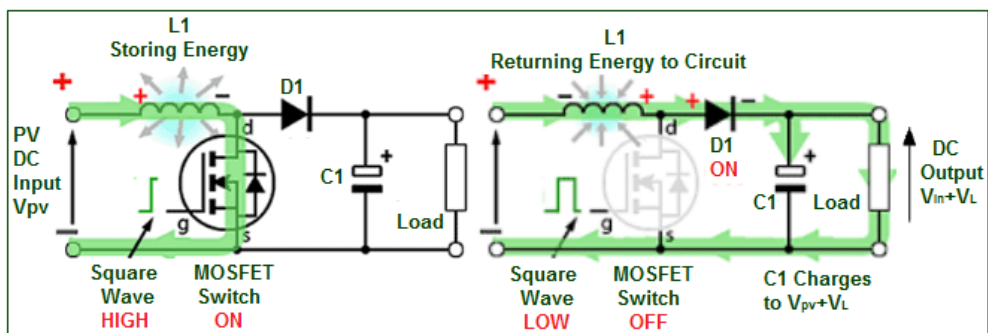


**Figure 5.** The two current paths of a boost converter, depending on the state of the switch S.

During the first mode, i.e. the ON-state when the switch is closed, the current will flow through the inductor in clockwise direction and the inductor will store the energy by generating a magnetic field. Thus, the polarity of the left side of the inductor is positive. During the second mode, i.e. the OFF-state when the switch is opened, the current will be reduced, due to the increase of impedance achieved during the first mode. The magnetic field previously created will be destroyed to maintain the current towards the load and thus, the polarity will be reversed and the left side of inductor will be negative. As a result, two sources will be in series causing a higher voltage to charge the capacitor through the diode D.

When the boost converter operates [12-13] in continuous mode, the current through the inductor  $I_L$  never falls to zero. Fig. 6 shows the typical waveforms of currents and voltages in a converter operating in this mode.

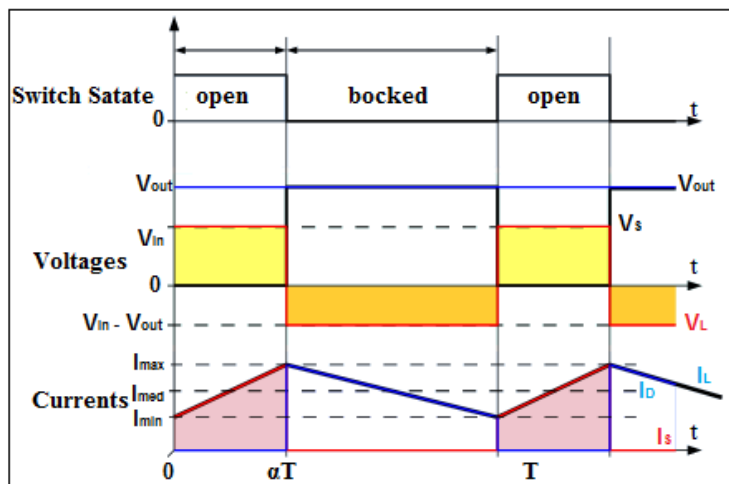


**Figure 6.** Waveforms of current and voltage in a boost converter operating in continuous mode.

During the ON-state, the change of the current  $I_L$  flowing through the inductor during a time period ( $t$ ) is described by the formula [14]:

$$\frac{\Delta I_L}{\Delta t} = \frac{V_{in}}{L} \quad (4)$$

At the end of the ON-state, the increase of  $I_L$  is therefore:

$$\Delta I_{Lon} = \frac{1}{L} \int_0^{\alpha T} V_{in} dt = \frac{\alpha T}{L} V_{in} \quad (5)$$

with  $\alpha$ , the duty cycle representing the fraction of the commutation period  $T$  during which the switch is ON. Therefore,  $D$  ranges between 0 (S is never ON) and 1 (S is always ON). During the OFF-state, the switch S is open, so the inductor current flows through the load. If we consider zero voltage drop in the diode, and a capacitor large enough for its voltage to remain constant, the evolution of  $I_L$  is:

$$V_{in} - V_{out} = L \frac{dI_L}{dt} \quad (6)$$

Therefore, the variation of  $I_L$  during the OFF-state is:

$$\Delta I_{Loff} = \int_{\alpha T}^T \frac{(V_{in}-V_{out})dt}{L} = \frac{(V_{in}-V_{out})(1-\alpha)T}{L} \quad (7)$$

As we consider that the converter operates in steady-state conditions, the amount of energy stored in each of its components has to be the same at the beginning and at the end of a commutation cycle. In particular, the energy stored in the inductor is given by:

$$E = \frac{1}{2} L I_L^2 \quad (8)$$

So, the inductor current has to be the same at the start and end of the commutation cycle. This means the overall change in the current (the sum of the changes) is zero:

$$\Delta I_{Lon} + \Delta I_{Loff} = 0 \quad (9)$$

It results:

$$\frac{V_{out}}{V_{in}} = \frac{1}{1-\alpha} \quad (10)$$

According to Eq. 10, the output voltage is always upper than that the input one. Thereby, the duty cycle value is the only variable that will allow us to control the output voltage. As we chose a boost converter system connected with a photovoltaic panel, the duty cycle value is calculated according to a mechanism named maximum power point tracking, MPPT. This one allows controlling the system and it makes their operation always optimal against environmental changes.

### The Photovoltaic Power Source

As the converter is dedicated to the conversion of energy coming from a photovoltaic source, we present in Fig. 7 the curves (I-V) and (P-V) of a PV panel. These curves allow to visualize the Maximum Power Point (MPP) at each changes of the available energy that continuously varies due to irradiation and temperature changes. Figure 6 also indicates the photovoltaic panel parameters, i.e. the MPP, the corresponding optimal voltage ( $V_M$ ) and optimal current ( $I_M$ ), the open circuit voltage ( $V_{OC}$ ), and the short circuit current ( $I_{SC}$ ).

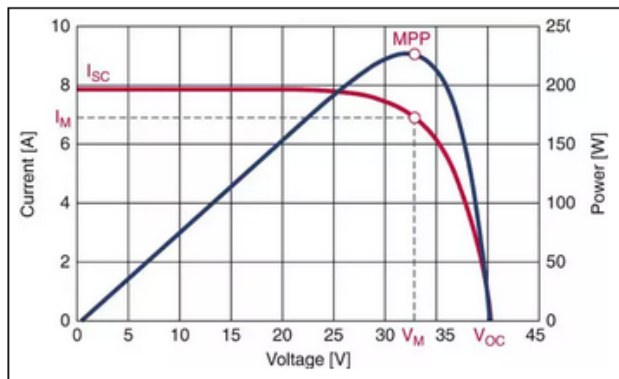


Figure 7. I-V and P-V characteristics for a photovoltaic panel.

## EXPERIMENTS

For experimentally illustrate the modeling of a coil dedicated to boost converter for photovoltaic functioning under real conditions, we have chosen a specific PV topology with common marketed elements. The type of the chosen photovoltaic panel to connect it with the system is a ZAYTECH 180S mono. It's composed of 72 mono-crystalline cells connected in a series/parallel topology according to the manufacturers' specification. The main elements of its technical sheet are reported on the following table [15].

TABLE 1. Characteristics of the panel ZAYTECH 180S mono.

$V_{oc}$	$I_{sc}$	$V_m(V)$	$I_m(A)$	$P_m(w)$	$T_{ref}(^{\circ}C)$	$E_{ref}(W/m^2)$
44.71	5.53	36.79	4.89	180	25	1000

### Realization and Characterization of the Coil

Manufacturers strive to realize elements whose inductive part is preponderant, according to major possible usages [16]. But it is impossible to realize a purely inductive element as modeled by the combine series/parallel model of the coil, Fig. 3. We represent in Fig. 8 the impedance module of an inductance coil as function of frequency (Hz), calculated with the model presented in Fig. 3.

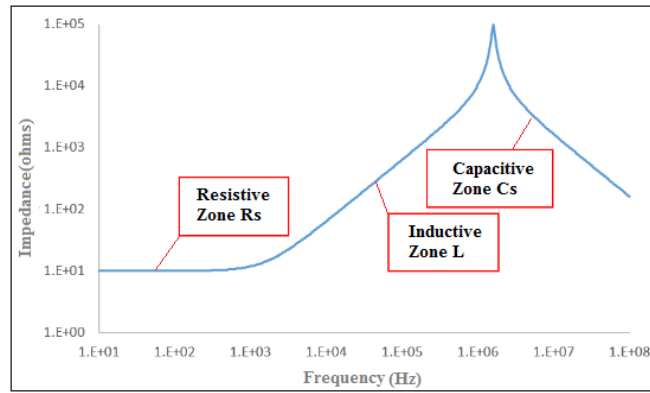


Figure 8. The module of the impedance  $Z$  of the coil.

According to the curve in Fig. 8, it is possible to define three zones: 1- The resistive zone characterized by the series resistance  $R_s$ . This value limits the maximum current in the inductance, therefore the energy that it is possible to store. 2- The inductive zone being characterized by the pure inductance  $L$ . This is the usual working zone of the inductor. 3- The capacitive zone is characterized by the capacity  $C_s$ . This zone is to avoid in practice since the inductor has an impedance that decreases as a function of frequency, which is the opposite effect of the desired one. Thereby, we note that the coil can never be purely inductive whatever the frequency used by the manufacturer.

To realize a coil dedicated to boost converter, we will follow the known steps cited in the literature [17-18] as well as in accordance to the international magnetic standards (ICS: 17.220) by respecting the impedance limit values indicated on the characteristic of Fig. 8. By else, to calculate the inductance value, the output parameters of the photovoltaic panel have to be considered as ideal. Among them a special attention needs to be done on the current  $I_M$  in order to avoid a spike of current that can afterwards gives us wrong values, on the joule effect losses of the coil conductor wire and on the magnetic interference that may adversely affect electronic components of the system.

When the optimal current provided by the PV panel is considered as ideal, we can note  $I_{pv} \max = I_M \cdot \sqrt{2}$ , knowing that  $I_{PV}=I_{IN}$  and  $V_{PV}=V_{IN}$ . We define  $\Delta I\%$  as the maximum variation of current in the inductance, thus given by the relation  $\Delta I_{pv} \max = I_{pv} \max * \Delta I\%$ . Currently  $\Delta I\%$  is imposed to be maximum equal to = 5%.

Within these parameters in Eq. 12, the inductance value  $L$  is defined as:

$$\Delta I_{pv \max} = \frac{V_{pv}}{L} \alpha_{\max} T \quad (11)$$

$$L = \frac{V_{pv} \cdot \alpha_{\max}}{\Delta I_{pv \max} \cdot f} \quad (12)$$

where  $V_{pv}$ (V) is the optimal voltage supplied by the photovoltaic panel,  $\alpha_{\max}$  is the value of the duty cycle allowing to obtain  $\Delta I_{pv \max}$ , and  $f$  is the switching frequency.

The basic material used for the torus is known under reference 3E25. This material was chosen as it reduces joule effect losses at high temperature, its frequency of use is between 10 kHz and 100 kHz, which corresponds to our application. Its toroid inductance,  $AL$  value is 3820 (nH/tr<sup>2</sup>). It is also necessary to provide a torus with a large diameter enough to pass the desired number of turns of the wire. Here, we have chosen a torus of dimensions 40x20x10 mm. To calculate the number of turns of the wire, we used the following equation

$$L = N^2 \cdot AL \quad (13)$$

According to the Eq.12 and 13 using the specific values of the input voltage provided by the PV panel ( $V_{pv}$ ), the maximal duty cycle ( $\alpha_{\max}$ ), the uncertainty of the maximum photovoltaic current ( $\Delta I_{pv \max}$ ), the frequency, the calculated inductance value ( $L$ ) and the toroid inductance value ( $AL$ ), we obtain the magnetic coil presented in Fig. 9.



**Figure 9.** Realized coil of 2,48 mH.

The coil presented in Fig. 9 was tested and characterized in the frequency band that can support the chosen torus model i.e. between 10 kHz, and 100 kHz. For these experiments, we have used a RLC METER (BENCHTOP 894 Series B&K Precision). The  $L(f)$  characteristic of the coil is plotted in Fig. 10.

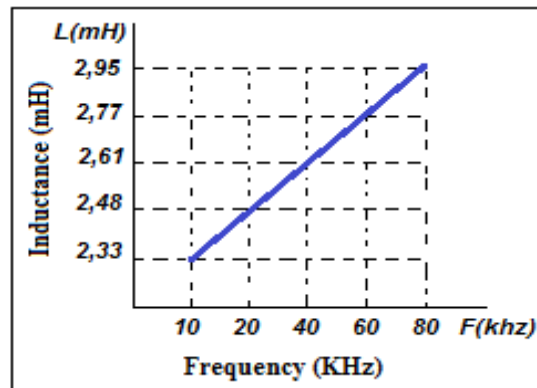


**Figure 10.** Frequency sweep and the influence of inductance.

We note in Fig. 10 that no saturation of the inductance value appears in the considered frequency range. In this range, the characteristic is proportionally positive with the frequency as expected by Eq. 12. This allows to have a precision at obtaining the experimental inductance value  $L$ .

### Characterization of the Converter Integrating the Coil and Discussions

For validating the sizing of the coil as function of parameters of the panel, we have simulated under Matlab/Simulink environment the efficiency of the converter by considering standard environmental conditions i.e. ambient temperature equal to 25°C and fixed irradiation equal to 1000W/m<sup>2</sup>. The output power, voltage and current are plotted in Fig. 11.

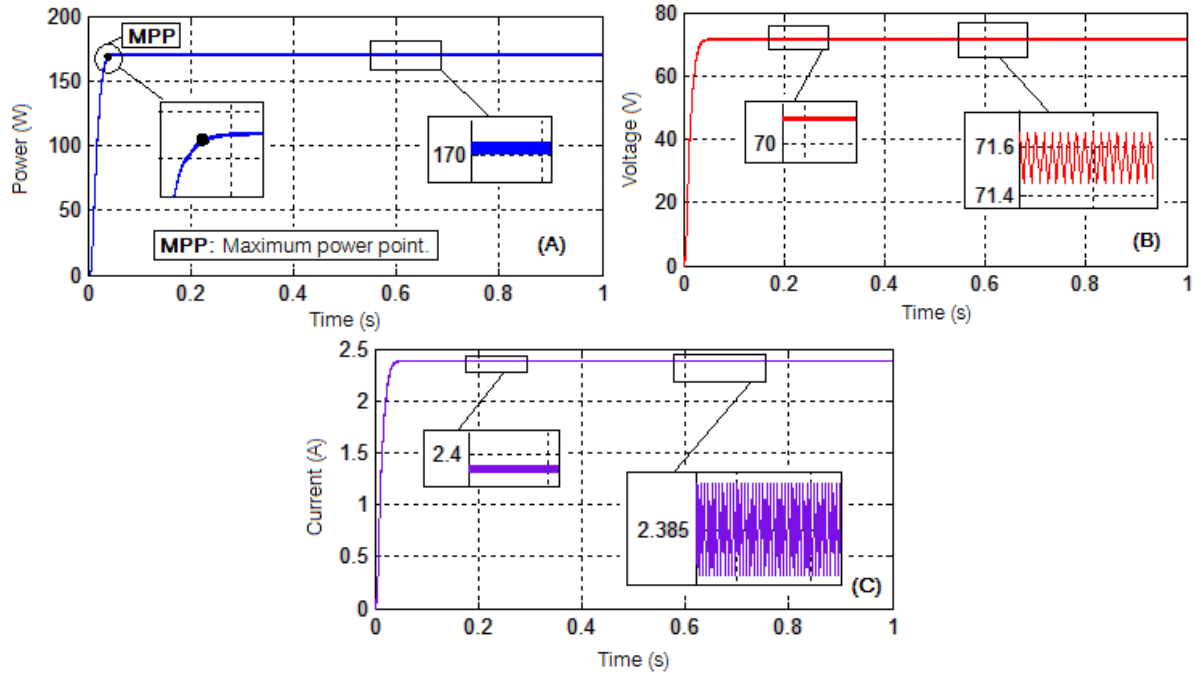


**Figure 11.** A) The output power  $P_s$ , B) voltage  $V_s$ , C) current  $I_s$  of the boost converter.

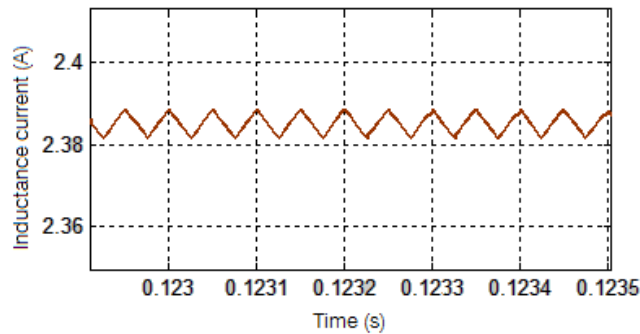


**Figure 12.** Current through the inductor  $i_L$ .

For a better visibility of the result, we chose a simulation time equal to 1 s. It is to be noted that the beginning of the experimental test does not correspond to practical situation but is actually proposed to simulate the influence of temperature and irradiation changes on PV generator. It avoids making long duration tests but it allows by extended the present simulating results, to simulate the output parameters of boost converter such as the power, voltage and current. Fig. 11.A shows the output power of the boost converter powered by a continuous photovoltaic source as a function of time. The temperature and irradiation are maintained fixe. A maximum power point tracking mechanism MPPT (the chosen algorithm is not presented here as it is out and independent of the scope of this contribution) is used to force the system to oscillate until it reached the MPP. At the steady

state, we noted that the average power is at 171 W compared to the power provided by the PV panel, which results in an excellent efficiency. According to Figs. 11, we note that the decrease of the output current resulting from the stored energy in the inductance L is proportional with the increase of the output voltage with respect of the photovoltaic panel parameters. The magnetic field created at the OFF-state will be destroyed to maintain the current to the load. The increase of the output voltage of the system is done when the switch is open as shown on Fig. 11. As a result, two sources will be in series causing a higher voltage to charge the capacitor through the diode D inducing the booster effect.

Fig. 12 shows the current through the inductance as a function of time. The current  $I_L$  presents sawtooth ripples called hysteresis form in literature, directly dependent of the ON-OFF state of the switch, thus always proportional to the duty cycle ( $\alpha$ ) when a boost converter operates in continuous mode corresponds to our case. In the current application, these ripples correspond to 0.22% of the inductance current  $I_L$ , which can be considered as a qualitative validation of the sizing of the coil.

## CONCLUSION

We have presented the various models and the sizing of coil integrated in boost converter which is one of the most popular converters topology as used in several applications and, as is concerned here, for maximum power delivery in renewable energy sources. After the presentation of the current models used for coils, we described the steps to realize an auto-inductor in accordance to the international magnetic standards (ICS: 17.220) by respecting the impedance limit values corresponding to a chosen torus models. Since our system is dedicated to photovoltaic, we have considered a marketed PV panel and we have presented the ON and OFF steps of the continuous operating mode of a boost converter using for that its equivalent electrical circuit. Lastly, a simulation results under (Matlab/Simulink) environment was presented of the output electrical parameters system such as power, voltage and current.

This contribution points the fact that, when the coil of a boost converter is well designed, the converter can ensure smooth operation with excellent performance when it is coupling to a PV panel and associate with an efficient maximum power point tracking process adapting the duty cycle of the boost's switch as function of irradiation and temperature variations. This demonstrates that the role of the coil is fundamental in boost converters determining the amplitude of the ripples of the electric current.

## REFERENCES

1. M. Marty, D. Dixneuf, D.G. Gilabert, *Principes d'électrotechnique – Cours et exercices corrigés* (Ed. Dunod, Paris, 2005).
2. M. Purhonen, J. Hannonen, J.P. Ström “Step-up DC-DC converter passive component dimensioning in photovoltaic applications”, *Electrical & Electronics Engineers in Israel* (2012).
3. P. Petit, M. Aillerie, T.V. Nguyen, J.P. Charles “Basic MOSFET Based vs Couple-coils Boost Converters for Photovoltaic Generators” *International Journal of Power Electronics and Drive Systems*, **4**(1), 1 (2014).
4. L. Atik, Z.T. Touhami. G. Bachir, J.P. Sawicki, P. Petit, M. Aillerie, “Comparison of four MPPT techniques for PV systems”, *AIP Conference Proceedings*, **1758**(1), 030047 (2016).
5. T.Z. Ternifi, L. Atik, G. Bachir, A.W. Belarbi, P. Petit, M. Aillerie, “Quality improvement of the AC electrical energy produced by a modular inverter dedicated to photovoltaic applications”, *AIP Conference Proceedings*, **1758**(1), 030048 (2016).
6. J.P. Ferrieux, F. Forest, *Alimentations à découpage, Convertisseurs à resonance* (Ed. Dunod, Paris, 3e edition, 1987).
7. Y. Li, C. Yang, Z. Yan, B. Guo, N. Mei, “Analysis of the icing and melting process in a coil heat exchanger”, *Energy Procedia* **136**, 450-455 (2017).
8. Y. Chen, H. Yang, “Thermal Performances Comparison between Dry-Coil and Wet-Coil Indirect Evaporative Cooler under the Same Configuration”, *Energy Procedia*, **75**, 3162-3167 (2015).
9. M.A. Fares, L. Atik, G. Bachir, M. Aillerie, “Photovoltaic panels characterization and experimental testing”, *Energy Procedia* **119**, 945-952 (2017).
10. G. Ang, P. J. Arcibal, L.M.R. Crisostomo, C.F. Ostia, P.J.C.S. Joaquin, J.E.C. Tabuton, “Implementation of a fuzzy controlled buck-boost converter for photovoltaic systems”, *Energy Procedia*, **143**, 641-648 (2017).

11. P. Petit, A. Zegaoui, J.P. Sawicki, M. Aillerie, J.P. Charles “New architecture for high efficiency DC-DC converter dedicated to photovoltaic conversion” [Energy Procedia](#), **6**, 688-694 (2011).
12. P. Petit, M. Aillerie, J-P. Sawicki, J-P. Charles “High efficiency DC DC converters including a performed recovering leakage energy switch” [Energy Procedia](#), **36**, 642-649 (2013).
13. P. Petit, M. Aillerie, J.P. Sawicki, T.V. Nguyen, J.P. Charles “Individual step-up converter with recovery stage for high efficiency conversion of photovoltaic energy”. [Energy Procedia](#), **50**, 479-487 (2014).
14. Z. Weiping, Z. Xiaoqiang, Z. Xusen, L. Yunchao “The dynamic analysis of power MOSFET in Buck converter. Power Electronics for Distributed Generation Systems (PEDG),” 2nd IEEE International Symposium (2010).
15. Y.P. Hsieh, J.F. Chen, T.J. Liang, L.S. Yang “A novel high step-up DC-DC converter for a microgrid system”, [IEEE Trans. On Power Electronics](#), **26**(4), 1127-1136 (2011).
16. N. Selvaraju, P. Shanmugham, S. Somkun, “Two-Phase Interleaved Boost Converter Using Coupled Inductor for Fuel Cell Applications”, [Energy Procedia](#), **138**, 199-204 (2017).
17. L. Atik, P. Petit, J.P. Sawicki, Z.T. Ternifi, G. Bachir, M. Della, M. Aillerie, “Maximum power point tracking algorithm based on sliding mode and fuzzy logic for photovoltaic sources under variable environmental conditions”, [AIP Conference Proceedings](#), 1814(1), 020063 (2017).
18. J.S. Jeon, S.R. Lee, “Suggestion of a Load Sharing Ratio for the Design of Spiral Coil-type Horizontal Ground Heat Exchangers”, [Energy Procedia](#), **141**, 292-298 (2017).